

Article

Fractional Modelling of H_2O_2 -Assisted Oxidation by Spanish broom peroxidase

Vinh Quang Mai ¹  and Thái Anh Nhan ^{2,*} 

¹ Department of Mathematics, Thu Dau Mot University, Thu Dau Mot 820000, Binh Duong, Vietnam; vinhmq@tdmu.edu.vn

² Department of Mathematics, Menlo College, 1000 El Camino Real, Atherton, CA 94027, USA

* Correspondence: anh.nhan@menlo.edu

Abstract: The H_2O_2 -assisted oxidation by a peroxidase enzyme takes place to help plants maintain the concentrations of organic compounds at physiological levels. Cells regulate the oxidation rate by inhibiting the action of this enzyme. The cells use two inhibitory processes to regulate the enzyme: a noncompetitive substrate inhibitory process and a competitive substrate inhibitory process. Numerous applications of peroxidase have been developed in clinical biochemistry, enzyme immunoassays, the treatment of waste water containing phenolic compounds, the synthesis of various aromatic chemicals, and the removal of peroxide from industrial wastes. The kinetic mechanism of the *Spanish broom peroxidase* enzyme is a Ping Pong Bi Bi mechanism with the presence of competitive inhibition by substrates. A mathematical model may help in identifying the key mechanism from amongst a set of competing mechanisms. In this study, we developed a fractional mathematical model to describe the H_2O_2 -supported oxidation by the enzyme *Spanish broom peroxidase*. Numerical simulations of the model produced results that are consistent with the known behaviour of *Spanish broom peroxidase*. Finally, some future investigations of the study are briefly indicated as well.

Keywords: competitive inhibition; noncompetitive inhibition; enzyme; fractional-order derivative; mathematical model; peroxidase

MSC: 92-10; 92B99; 92C45; 92E20



Citation: Mai, V.Q.; Nhan, T.A.

Fractional Modelling of H_2O_2 -Assisted Oxidation by *Spanish broom peroxidase*. *Mathematics* **2024**, *12*, 1411. <https://doi.org/10.3390/math12091411>

Academic Editor: Ioannis K. Argyros

Received: 29 March 2024

Revised: 1 May 2024

Accepted: 2 May 2024

Published: 5 May 2024



Copyright: © 2024 by the authors. Licensee MDPI, Basel, Switzerland. This article is an open access article distributed under the terms and conditions of the Creative Commons Attribution (CC BY) license (<https://creativecommons.org/licenses/by/4.0/>).

1. Introduction

Enzymes, natural proteins found in living organisms, catalyse biochemical reactions essential for cell metabolism by reducing the activation energy. They are not consumed during reactions and can be biologically degradable, suggesting an important role in environmental protection [1–5]. Cells regulate metabolite concentrations through various mechanisms, including enzymatic inhibition processes such as competitive, noncompetitive, and uncompetitive inhibition. Competitive inhibition involves substrate and inhibitor molecules competing for enzyme binding sites, hindering catalytic activity. The competitive substrate inhibition of an enzyme is a competitive inhibition process in which the substrate plays the role of inhibitor, and enzymes often are bi-substrate enzymes. Some enzymes, for example, *Spanish broom peroxidase*, can be inhibited by their substrates [6,7].

Enzymes offer numerous benefits due to the features of enzymes. Nowadays, scientific and technological advances facilitate studies on enzymes and their applications [6–8]. Novel enzymes are increasingly being extracted and investigated. A variety of applications of enzymes have been developed for biotechnology, industry, and medicine. Some common applications of enzymes take place in pharmaceuticals, food processing, biofuels, and so on [8–11]. Understanding enzyme mechanisms is crucial for application development, utilising both experimental and mathematical modelling approaches [12–17].

Plants use oxygen as a terminal electron acceptor. Class III plant peroxidases (EC 1.11.1.7; donor: hydrogen peroxide oxidoreductases) help maintain low levels of hydrogen

peroxide [18]. Peroxidases are enzymes that catalyse the oxidation of numerous substrates such as halide, aromatic amines, phenols, and thiosanisoles through H_2O_2 reduction. The reducing substrate is dependent on the type of peroxidase enzyme [19]. Enzymatic biocatalysis plays a crucial role in the development of many chemical industries. Due to the catalytic features of peroxidases, they become attractive enzymes for biotechnological processes. Investigating substrate specificity and the effectors affecting peroxidase enzyme activities may assist in developing the use of the catalytic potential of peroxidases [20]. Peroxidases also play important roles in clinical biochemistry and enzyme immunoassays [21]. Recently, peroxidases were used in the treatment of waste water containing phenolic compounds, the synthesis of various aromatic chemicals, and the removal of peroxide from industrial wastes [22].

In recent years, experimental evidence has increasingly pointed to the relevance of fractional calculus analysis in understanding dynamic phenomena in nature. This burgeoning field of research has seen rapid growth, driven by its wide-ranging applications across diverse areas of engineering and science. From chemical models to physics and signal and image processing to quantum mechanics and control theory to nonlinear dynamics, fractional calculus finds utility in a multitude of disciplines. Furthermore, its application extends to biological population models, optimisation theory, and beyond [23–28].

Alicea [29] and Alawneh [30] independently tackled the integer order-model for the system of the following chemical reaction:



using different mathematical methods. Alicea employed the method of multiple time scales to obtain asymptotic solutions, while Alawneh utilised a generalised differential transform method with multisteps and discussed estimation analysis using fractional order derivatives. However, despite their efforts, the solutions obtained mathematically for the concentrations of E , S , ES , and P at any time t often did not align with those of the experimental results. To address this discrepancy, alternative approaches have been explored, including the use of fractional derivatives instead of integer-order derivatives. Fractional derivatives offer greater flexibility and accuracy compared to classical derivatives, making them particularly appealing for modelling complex systems. Interested readers are encouraged to explore the works referenced in [26,31] for further insights into the advantages of fractional derivatives in mathematical modelling.

In this study, we developed a fractional mathematical model describing hydrogen peroxide-assisted oxidation by *Spanish broom peroxidase* enzyme. The model consists of the *Spanish broom peroxidase* enzyme, the substrates H_2O_2 and AH_2 , and their complexes. Numerical simulations provided insights into the model behaviour, using Python software for numerical integration. The notations employed in subsequent sections are elucidated in Figure 1.

The rest of this paper is organised as follows. In Section 2, we describe the formulation of the mathematical model and methods used in the current study. Numerical solutions for the model are presented in Section 3. Finally, we discuss some concluding remarks in Section 4.

NOMENCLATURE	
$[X]$	– the concentration of a species X ; a function of time (mM)
E	– a molecule of the enzyme
E'	– a molecule of the intermediate enzyme
H_2O_2	– a molecule of the substrate H_2O_2
AH_2	– a molecule of the substrate AH_2 (Ferulic acid, Guaiacol, Catechol, etc.)
H_2O	– a molecule of the product H_2O
AH^\bullet	– a molecule of the product AH^\bullet
$E \cdot H_2O_2$	– an enzyme- H_2O_2 complex
$E' \cdot AH_2$	– an intermediate enzyme- AH_2 complex
$E \cdot AH_2$	– an enzyme- AH_2 complex
$E \cdot AH^\bullet$	– an enzyme- AH^\bullet complex
$E' \cdot H_2O_2$	– an intermediate enzyme- H_2O_2 complex
k_4	– catalytic rate for the intermediate enzyme acting on a substrate molecule AH_2 (s^{-1})
k_1	– adsorption rate of substrate molecules H_2O_2 to free enzyme molecules E ($mM^{-1}s^{-1}$)
k_{-1}	– desorption rate of substrate molecules from enzyme-substrate complexes $E \cdot H_2O_2$ (s^{-1})
k_2	– catalytic rate for the enzyme acting on a substrate molecule H_2O_2 (s^{-1})
k_3	– adsorption rate of substrate molecules AH_2 to free intermediate enzyme molecules E' ($mM^{-1}s^{-1}$)
k_{-3}	– desorption rate of substrate molecules AH_2 from enzyme-substrate complexes $E' \cdot AH_2$ (s^{-1})
k_5	– adsorption rate of substrate molecules AH_2 to free enzyme molecules E ($mM^{-1}s^{-1}$)
k_{-5}	– desorption rate of substrate molecules AH_2 from enzyme-substrate complexes $E \cdot AH_2$ (s^{-1})
k_6	– adsorption rate of substrate molecules H_2O_2 to free intermediate enzyme molecules E' ($mM^{-1}s^{-1}$)
k_{-6}	– desorption rate of substrate molecules H_2O_2 from enzyme-substrate complexes $E' \cdot H_2O_2$ (s^{-1})

Figure 1. Notations and their descriptions.

2. Materials and Methods

2.1. Mathematical Model

In this section, we present a minimal fractional-order model that describes the H_2O_2 -assisted oxidation by *Spanish broom peroxidase* enzyme, in which the substrates competitively inhibit the enzyme by binding to the enzyme molecule at the binding site for the other substrate. The fractional derivative operator, which is used in this study, is the Caputo one.

The fractional derivative of order α in the Caputo sense is defined as the operator $D_t^\alpha f(t)$ such that

$$D_t^\alpha f(t) = \frac{1}{\Gamma(m - \alpha)} \int_0^t \frac{f^{(m)}(s)}{(t - s)^{\alpha + 1 - m}} ds, \quad m - 1 < \alpha < m,$$

where Γ is the Gamma function defined as follows:

$$\Gamma(\alpha) = \int_0^\infty u^{\alpha - 1} e^{-u} du, \quad \alpha > 0.$$

Here, we list several common formulae for the Gamma function as follows:

$$\begin{aligned} \Gamma(\alpha + 1) &= \alpha \Gamma(\alpha), \\ \Gamma(\alpha + n) &= \alpha(\alpha + 1) \cdots (\alpha + n - 1) \Gamma(\alpha), \\ \Gamma(n + 1) &= (n + 1)!, \quad n = 0, 1, 2, \dots, \\ \Gamma(\alpha) \Gamma(1 - \alpha) &= \frac{\pi}{\sin(\pi \alpha)}. \end{aligned}$$

For more details, the readers can find them in [32]. In the current study, we used $\alpha \in (0, 1)$. Next, we provide a brief description of the kinetic mechanism that the model was based on.

2.1.1. The Kinetic Mechanism

It is known that *Spanish broom peroxidase* catalyses the H_2O_2 -mediated oxidation in a Ping Pong mechanism with the presence of competitive inhibition by the substrates [6]. The kinetic mechanism for the H_2O_2 -mediated oxidation by *Spanish broom peroxidase* is summarised in Figure 2.

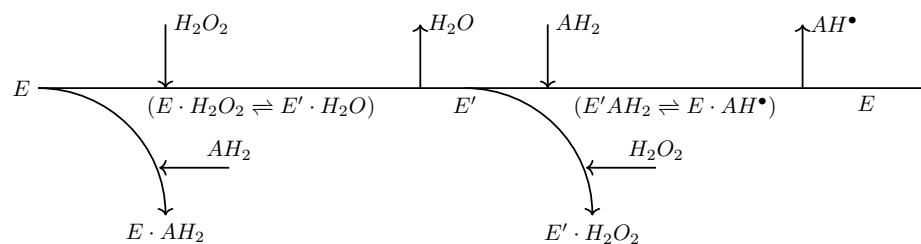


Figure 2. Diagram of Ping Pong mechanism with competitive inhibition by the substrates. Here E represents an molecule of *Spanish broom peroxidase* enzyme, H_2O_2 and AH_2 are the substrates molecules, H_2O and AH^\bullet are the products molecules. Further, E' corresponds to an intermediate enzyme molecule, $E \cdot H_2O_2$, $E' \cdot AH_2$, $E \cdot AH_2$, $E' \cdot H_2O_2$ substrate-enzyme complexes, and $E' \cdot H_2O$, $E \cdot AH^\bullet$ product-enzyme complexes.

For convenience, the mechanism in Figure 2 can be illustrated using separated stages as in Figure 3.

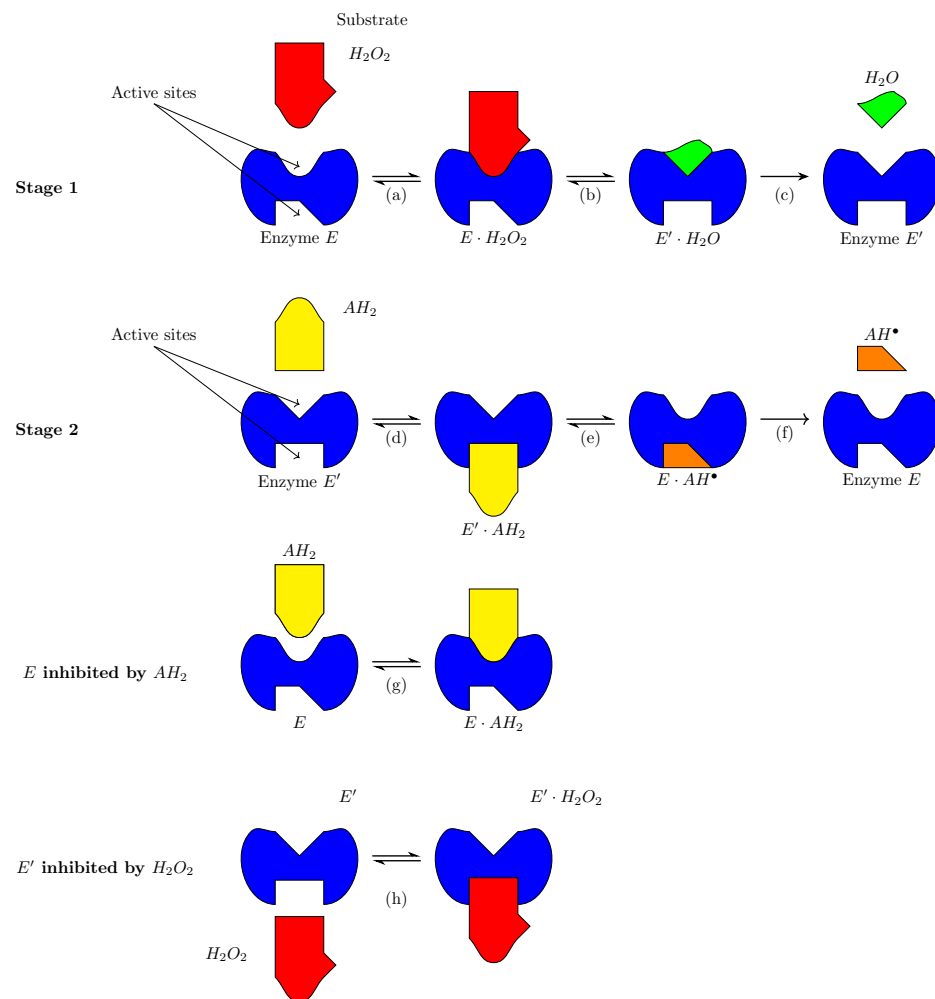


Figure 3. Illustration of a Ping Pong mechanism with the inhibition by substrates. A double arrow represents a reversible reaction, whereas a single arrow corresponds to an irreversible reaction. In Stage 1, (a) an H_2O_2 substrate molecule binds to a free enzyme molecule E to form an enzyme–substrate complex molecule $E \cdot H_2O_2$, (b) the bound enzyme molecule E catalyses the reactions to convert a substrate molecule H_2O_2 into an H_2O product molecule and an intermediate form E' , and (c) the intermediate enzyme molecule releases the product molecule to the medium. In Stage 2, (d) an AH_2 substrate molecule binds to a free intermediate enzyme molecule E' to form an enzyme–substrate complex molecule, (e) the bound intermediate enzyme molecule catalyses specific reactions to convert a AH_2 substrate molecule into a product molecule AH^\bullet and recover to an original enzyme molecule E , and (f) the original enzyme molecule irreversibly releases the product molecule AH^\bullet to the medium. In (g), an AH_2 substrate molecule temporarily inhibits a free original enzyme molecule by binding to the binding site of the enzyme molecule for H_2O_2 substrate molecules (competitive inhibition). Finally, (h) displays an H_2O_2 substrate molecule that competitively inhibits a free intermediate enzyme molecule E' (reversibly) by binding to the binding site of the enzyme molecule for AH_2 substrate molecules.

In this mechanism, an enzyme molecule has at least two binding sites for its substrates and produces two types of product molecules. The Ping Pong mechanism includes two stages: Stage 1 and Stage 2. In Stage 1, an enzyme molecule E absorbs a molecule of substrate H_2O_2 to form a substrate–enzyme complex $E \cdot H_2O_2$. The bound enzyme molecule catalyses the complex to form a product–enzyme complex $E' \cdot H_2O$. It should be noticed that these reactions are reversible reactions. Then, the enzyme releases the

product molecule H_2O and an intermediate enzyme molecule E' into the medium. This is an irreversible reaction.

When intermediate enzyme molecules E' occur at the end of Stage 1, each of them may be able to initiate Stage 2 by absorbing a substrate molecule AH_2 to form a substrate–enzyme complex $E' \cdot AH_2$. The bound enzyme molecule catalyses the complex $E' \cdot AH_2$ to form a product–enzyme complex $E \cdot AH^\bullet$. These reactions are reversible also. The product molecule AH^\bullet and original enzyme molecule E are then irreversibly released into the medium.

The competitive inhibition by the substrates includes the inhibition by H_2O_2 and the inhibition by AH_2 . First, we explain the competitive inhibition by substrate H_2O_2 . The inhibition is interpreted as follows: a substrate molecule H_2O_2 that is able to bind to an enzyme molecule E' to form a substrate–enzyme complex $E' \cdot H_2O_2$. The binding of a molecule H_2O_2 to an enzyme molecule E' prevents the AH_2 molecules from binding to the enzyme molecule E' [6,33,34].

The competitive inhibition by the substrate AH_2 is represented as follows: a substrate molecule AH_2 that is capable of binding to an enzyme molecule E to form a substrate–enzyme complex $E \cdot AH_2$. The binding of a molecule AH_2 to an enzyme molecule E prevents H_2O_2 molecules from binding to the enzyme molecule E [6,33,34].

To simplify the modelling, we reduced the above kinetic mechanism using a minimal set of chemical reactions as follows (Figure 4).

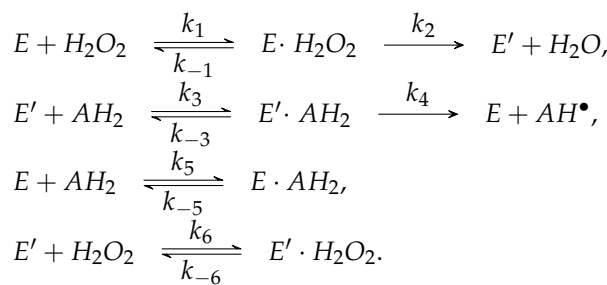


Figure 4. A simplified scheme of the Ping Pong mechanism. The notations used here are the same as those in Figure 2. Furthermore, the parameter k_i s are the constant rates of the chemical reactions. See the Nomenclature for more details.

Assumptions are needed for developing a mathematical model. In the next section, we list some assumptions for the model.

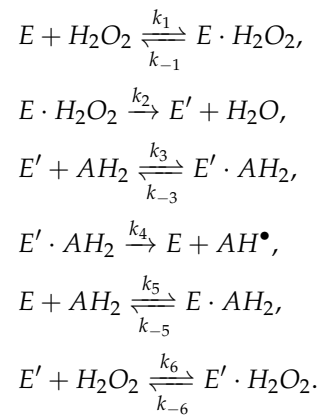
2.1.2. Modelling Assumptions

The model developed here was based on the law of mass action. The system is quite complex due to the number of binding sites of an enzyme molecule. Here are the necessary assumptions for the model.

- The mixture of peroxidase enzyme, H_2O_2 , and AH_2 (such as Ferulic acid, Guaiacol, Catechol, etc.) is well stirred throughout. This implies that diffusive effects in the process can be omitted and that the concentrations of the various species in the mixture can be described by functions of time only. This further implies that the evolution of the system can be modelled using a coupled system of nonlinear fractional differential equations and that a partial differential equation model is not required [15,35].
- We assume that mass action kinetics occur throughout; this implies that the rate of a reaction is taken to be proportional to the product of the concentrations of the reactants. We emphasise here that more complex formulas, such as the Michaelis–Menten formula for the rate of product formation in an enzyme-catalysed reaction, are derivable from more fundamental mass action considerations under simplifying assumptions [15,35].

2.1.3. Construction of the Governing Fractional Differential Equations

For the convenience of modelling, we can rewrite the chemical reactions in Figure 4 as follows:



Under the above assumptions and using the law of mass action, the model equations that describe the concentrations of the species in the mixture are given by

$$D_t^\alpha [E] = -k_1[E][H_2O_2] - k_5[E][AH_2] + k_{-1}[E \cdot H_2O_2] + k_4[E' \cdot AH_2] + k_{-5}[E \cdot AH_2], \quad (2)$$

$$D_t^\alpha [H_2O_2] = -k_1[E][H_2O_2] - k_6[E'][H_2O_2] + k_{-1}[E \cdot H_2O_2] + k_{-6}[E' \cdot H_2O_2], \quad (3)$$

$$D_t^\alpha [E \cdot H_2O_2] = -(k_{-1} + k_2)[E \cdot H_2O_2] + k_1[E][H_2O_2], \quad (4)$$

$$\begin{aligned}
 D_t^\alpha [E'] &= -k_3[E'][AH_2] - k_6[E'][H_2O_2] + k_2[E \cdot H_2O_2] \\
 &\quad + k_{-3}[E' \cdot AH_2] + k_{-6}[E' \cdot H_2O_2],
 \end{aligned} \quad (5)$$

$$D_t^\alpha [H_2O] = k_2[E \cdot H_2O_2], \quad (6)$$

$$D_t^\alpha [AH_2] = -k_3[E'][AH_2] - k_5[E][AH_2] + k_{-3}[E' \cdot AH_2] + k_{-5}[E \cdot AH_2], \quad (7)$$

$$D_t^\alpha [E' \cdot AH_2] = -(k_{-3} + k_4)[E' \cdot AH_2] + k_3[E'][AH_2], \quad (8)$$

$$D_t^\alpha [AH^\bullet] = k_4[E' \cdot AH_2], \quad (9)$$

$$D_t^\alpha [E \cdot AH_2] = -k_{-5}[E \cdot AH_2] + k_5[E][AH_2], \quad (10)$$

$$D_t^\alpha [E' \cdot H_2O_2] = -k_{-6}[E' \cdot H_2O_2] + k_6[E'][H_2O_2], \quad (11)$$

where $[X] = [X](t)$ denotes the concentration of species X at time t .

It is not necessary to provide discussions of these equations here. However, we do briefly discuss two of them to illustrate how the model equations are constructed. The chemical reactions for the model are displayed in Figure 4. We begin by considering the Equation (2) for E given by

$$D_t^\alpha [E] = \underbrace{-k_1[E][H_2O_2]}_1 - \underbrace{k_5[E][AH_2]}_2 + \underbrace{k_{-1}[E \cdot H_2O_2]}_3 + \underbrace{k_4[E' \cdot AH_2]}_4 + \underbrace{k_{-5}[E \cdot AH_2]}_5,$$

where the numbered parts are described as follows:

- 1 This term accounts for the reduction in the concentration of E due to substrate H_2O_2 binding.
- 2 The reduction in the concentration of E due to substrate AH_2 binding.

- 3 The increase in the concentration of E due to the substrate unbinding from the complex $E \cdot H_2O_2$.
- 4 The increase in the concentration of E due to the enzyme catalysing the complex $E' \cdot AH_2$ and releasing the product and the original enzyme molecule.
- 5 The increase in the concentration of E due to the substrate unbinding from the complex $E \cdot AH_2$.

Now, we turn our attention to Equation (4) for complex $E \cdot H_2O_2$:

$$D_t^\alpha [E \cdot H_2O_2] = \underbrace{-(k_{-1} + k_2)[E \cdot H_2O_2]}_a + \underbrace{k_1[E][H_2O_2]}_b,$$

where the parts are as follows:

- a This accounts for the reduction in the concentration of $E \cdot H_2O_2$ due to the substrate unbinding from $E \cdot H_2O_2$ and the enzyme catalysing $E \cdot H_2O_2$ to form product H_2O .
- b The increase in the concentration of $E \cdot H_2O_2$ due to the enzyme binding to the substrate H_2O_2 .

The remaining equations, Equations (3) and (5)–(11), are interpreted similarly.

2.1.4. Initial Conditions

The equations described in the previous subsection are solved under the initial conditions:

$$\begin{aligned} [E](t = 0) &= e_0 \text{ mM}, & [E'](t = 0) &= 0.0 \text{ mM}, \\ [H_2O_2](t = 0) &= a_0 \text{ mM}, & [AH_2](t = 0) &= b_0 \text{ mM}, \\ [E \cdot H_2O_2](t = 0) &= 0.0 \text{ mM}, & [E' \cdot AH_2](t = 0) &= 0.0 \text{ mM}, \\ [H_2O](t = 0) &= 0.0 \text{ mM}, & [AH^\bullet](t = 0) &= 0.0 \text{ mM}, \\ [E \cdot AH_2](t = 0) &= 0.0 \text{ mM}, & [E' \cdot H_2O_2](t = 0) &= 0 \text{ mM}, \end{aligned}$$

where e_0 , a_0 , and b_0 give the initial constant concentrations of the enzyme, H_2O_2 , and AH_2 , respectively. The initial concentrations for all of the enzyme complexes were taken to be zero. Finally, the initial concentrations of the rest of the species were set to be zero also.

2.1.5. Conservation Laws

Computing the sum of Equations (2) + (4) + (5) + (8) + (10) + (11), (3) + (4) + (6) + (11) and (7) + (8) + (9) + (10) and integrating both sides yields

$$[E] + [E \cdot H_2O_2] + [E'] + [E' \cdot AH_2] + [E \cdot AH_2] + [E' \cdot H_2O_2] = e_0, \tag{12a}$$

$$[H_2O_2] + [E \cdot H_2O_2] + [H_2O] + [E' \cdot H_2O_2] = a_0, \tag{12b}$$

$$[AH_2] + [E' \cdot AH_2] + [AH^\bullet] + [E \cdot AH_2] = b_0, \tag{12c}$$

which are the expressions of the conservation of enzyme E and substrates H_2O_2 and AH_2 , respectively.

2.2. Computational Methods

In this section, we describe the computational tools used to analyse the model equations. The software developed for this paper was coded using the Python programming language [36].

2.2.1. Numerical Method for Solving the Fractional Differential Equations

The numerical integration of fractional-order ordinary differential equations was performed using the `fodeint` solver, alongside the SciPy and Numpy libraries [37–39]. SciPy [39] is an open-source Python [36] library that provides numerical routines for scientific and engineering applications. The `fodeint` solver, a Python package, numerically integrates fractional ordinary differential equations using an explicit one-step Adams–

Bashforth (Euler) method [40,41]. However, the convergence and accuracy of this method have not yet been evaluated. Recently, novel numerical methods have been developed to solve fractional-order ordinary differential equations efficiently, and their analyses have yielded several interesting results [42,43]. The employment of these methods in creating a new Python solver for fractional-order ordinary differential equations could lead to intriguing research opportunities. In the present study, our primary aim involved investigating a specific phenomenon utilising well-established methodologies, including theoretical frameworks and computational libraries. Our focus did not extend to creating a computational library specifically for solving non-integer differential equations. Nevertheless, we maintained an open-minded approach and may consider exploring such endeavors opportunistically in the days ahead.

2.2.2. Model Parameter Values

Table 1 shows some of the model parameter values, together with their literature sources. Typically, the parameter values are rare in the literature, except a few of them.

Table 1. Some model parameter values and their literature sources.

Parameter	Value	Unit	Ref.
k_1	9.1	$\text{mM}^{-1}\text{s}^{-1}$	
k_{-1}	3.2	s^{-1}	
k_2	14.5	s^{-1}	
k_3	9.8	$\text{mM}^{-1}\text{s}^{-1}$	
k_{-3}	2.4	s^{-1}	
k_4	12.6	s^{-1}	[6]
k_5	8.0	$\text{mM}^{-1}\text{s}^{-1}$	
k_{-5}	2.5	s^{-1}	
k_6	7.0	$\text{mM}^{-1}\text{s}^{-1}$	
k_{-6}	1.5	s^{-1}	

3. Results and Discussion

3.1. Numerical Results

The Section 2 introduced the mathematical model. It also described the computational methods used to integrate the model equations, and included some discussion of the numerical method, the choice of parameter values, and the initial conditions. In the current section, we describe some of the numerical results obtained some initial conditions. The initial conditions used here correspond to $e_0 = 5.0 \text{ mM}$, $a_0 = 9.0 \text{ mM}$, and $b_0 = 15.0 \text{ mM}$; see Section 2.1.4 for details.

The principal purpose of the numerical solutions displayed here was to gain insight into the H_2O_2 -assisted oxidation by *Spanish broom peroxidase*. To focus attention on the oxidation process itself, we made no attempt to model the evolution of the physiological levels of the species in the mixture. Instead, we simply assumed the constant initial concentrations of the species and then tracked its subsequent conversion via the enzymatic reactions. It should be noted that the derivative order used here was $\alpha = 0.8$. The nearer to zero that the α is, the longer the time consumption for the computation.

In Figure 5, we plotted the numerical solutions of the model corresponding to the initial conditions and the parameter values aforementioned. Each line corresponds to the concentration of one species in the mixture with respect to time t . Some points of discussion on these numerical results are as follows.

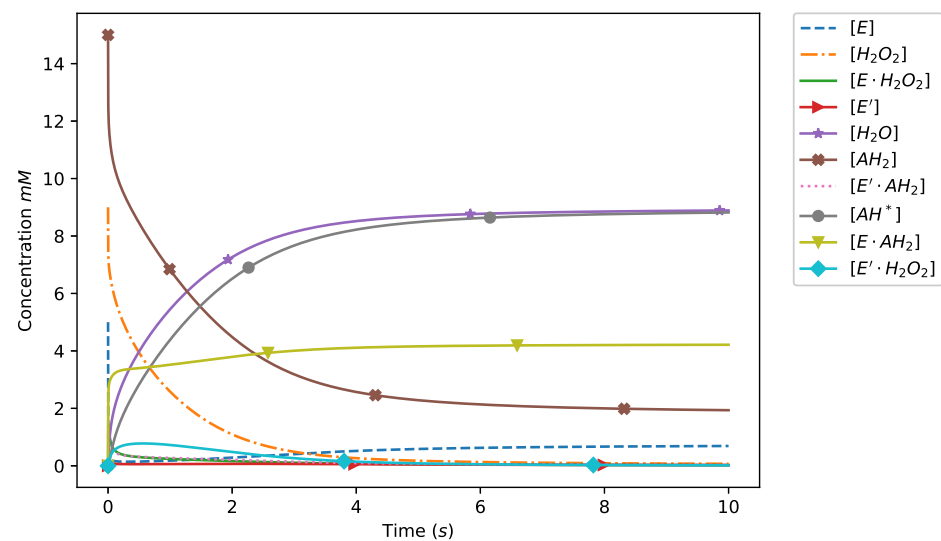


Figure 5. Numerical solutions of the model. Each line represents the concentration of one species in the mixture with respect to t . The values of the model parameters are referred to in the main text. Similarly, the initial conditions of the model are also presented in the main text.

- The line $\text{---}\text{---}\text{---}\text{---}$ represents the concentration of the enzyme during the process. In the first stage, the concentration of enzyme drops rapidly due to the binding of substrates to form substrate–enzyme complexes $E \cdot H_2O_2$ and $E \cdot AH_2$. As time goes on, the enzyme converts the substrates to products. This reduces the concentrations of the substrates and makes the increases in the concentrations of products continuous. The concentration of the enzyme goes up and reaches a steady state at the end of the process. It should be noted that the steady concentration of the enzyme is lower than its initial concentration.
- The line $\text{---}\text{---}\text{---}\text{---}$ displays the concentration of the substrate H_2O_2 . The concentration decreases rapidly and reaches a steady state at the end of the process. This occurs because the intermediate enzyme E' cannot convert the product H_2O to the substrate H_2O_2 .
- The line $\text{---}\text{---}\text{---}\text{---}$ describes the concentration of the substrate–enzyme complex $E \cdot H_2O_2$. It can be seen that the concentration rises up rapidly in the early stage because of the binding of the substrate to the enzyme. Then, the concentration drops down quickly since the enzyme catalyses the complex to form product H_2O , and the substrate unbinds from the complex. In the end, the concentration of the complex is completely catalysed to form the product H_2O and tends to zero then. This is because the reaction is irreversible.
- The line $\text{---}\text{---}\text{---}\text{---}$ corresponds to the concentration of the intermediate enzyme E' . The concentration increases gradually and tends to zero at the end of the process. This agrees with the nature of the process. That is, the intermediate enzyme is incapable of converting the product H_2O to the substrate H_2O_2 and the original enzyme E , and the substrate AH_2 binds to the enzyme E' to form complexes $E' \cdot AH_2$.
- The line $\text{---}\text{---}\text{---}\text{---}$ shows the concentration of the product H_2O . The concentration increases rapidly and reaches a steady state. It is clear that the concentration approaches the initial concentration of the substrate H_2O_2 . In the end, the substrate H_2O_2 is completely converted to the product H_2O . This is in line with the nature of the process since the enzyme is not able to convert the product H_2O to the substrate H_2O_2 .
- The line $\text{---}\text{---}\text{---}\text{---}$ represents the concentration of the substrate AH_2 . The rapid decrease in the concentration of AH_2 is due to the binding of the substrate AH_2 to the intermediate enzyme E' to form the substrate–enzyme complex $E' \cdot AH_2$. The concentration tends to the concentration of H_2O at the end of the process since this process will not

take place once the substrate H_2O_2 is completely consumed. This agrees with the fact that the enzyme is not able to convert the product AH^\bullet to the substrate AH_2 at all.

- The line shows the concentration of the substrate–enzyme complex $E' \cdot AH_2$. At the early stage, the rapid increase in the concentration is due to the binding of the substrate AH_2 to the intermediate enzyme E' to form the complex $E' \cdot AH_2$. The concentration approaches zero at the end of the process since the complex is totally catalysed to form the product AH^\bullet , and the substrate AH_2 is completely converted to the product AH^\bullet . This is in line with the fact that the conversion of the complex to the product AH^\bullet is an irreversible reaction.
- The line —●— displays the concentration of the product AH^\bullet with respect to time t . The concentration increases quickly at the early stage since the concentration of the complex $E' \cdot AH_2$ increase quickly and the enzyme rapidly catalyses the complex and releases the product then. The concentration tends to the initial concentration of the substrate AH_2 or that of H_2O_2 . The reason is that the reactions that form the product AH_2 will be terminated at once if the substrate H_2O_2 or AH_2 is exhausted.
- The line —▲— shows the concentration of the substrate–enzyme complex $E \cdot AH_2$. At the early stage, the rapid increase in the concentration is due to the binding of the substrate AH_2 to the enzyme E to form the complex $E \cdot AH_2$. It should be noted that this reaction is reversible. The concentration approaches a steady state at the end of the process since the substrate H_2O_2 is completely converted to the product H_2O . This means that the enzyme E' is exhausted.
- The line —◆— displays the concentration of the substrate–enzyme complex $E' \cdot H_2O_2$. At the early stage, the increase in the concentration is due to the binding of the substrate H_2O_2 to the enzyme E' to form the complex $E' \cdot H_2O_2$. It should be noted that this reaction is reversible. The concentration tends to zero at the end of the process since the substrate H_2O_2 is completely converted to the product H_2O .

3.2. Further Numerical Results

We now display some further numerical solutions inspired by the fact that the fractional order α is in $(0, 1)$. That is, we conducted some numerical experiments for the different values of α to obtain insights into the behaviours of the solutions of the model. These values of α were taken to be $\alpha = 0.7$, $\alpha = 0.8$, and $\alpha = 0.9$ to reduce the computation time. In these calculations, the default values used for the parameters are shown in Table 1, and the initial concentrations for the enzyme, H_2O_2 , and AH_2 are those used in Section 3.1. We used the solutions of the model for the product H_2O and the substrate AH_2 for this investigation.

In Figure 6, the solutions of the model for the product H_2O were used to study $\alpha = 0.7$, $\alpha = 0.8$, and $\alpha = 0.9$. We illustrate how the new numerical results shown in Figure 6 were generated by considering a particular example. Here, we consider the curves displayed in Figure 6. The solid blue curve was generated using $\alpha = 0.7$. The solid orange curve was generated using $\alpha = 0.7$, and the dash–dot green curve was generated using $\alpha = 0.9$. It can be clearly seen that the higher the value of α , the faster the increase in the concentration of H_2O .

Figure 7 shows the plots of the concentrations of AH_2 with respect to time t for different values $\alpha = 0.7$, $\alpha = 0.8$, and $\alpha = 0.9$. Clearly, the smaller the value of α , the slower the decrease in the concentration of AH_2 .

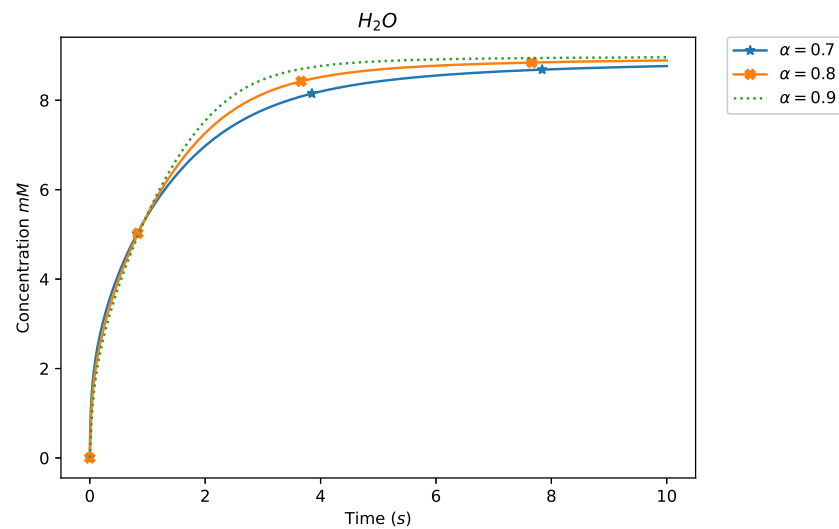


Figure 6. Numerical solutions of the model for the concentration of H_2O . Each line represents the concentration of H_2O in the mixture with respect to t for different values $\alpha = 0.7$, $\alpha = 0.8$, and $\alpha = 0.9$. The values of the model parameters are in the main text. Similarly, the initial conditions of the model are also presented in the main text.

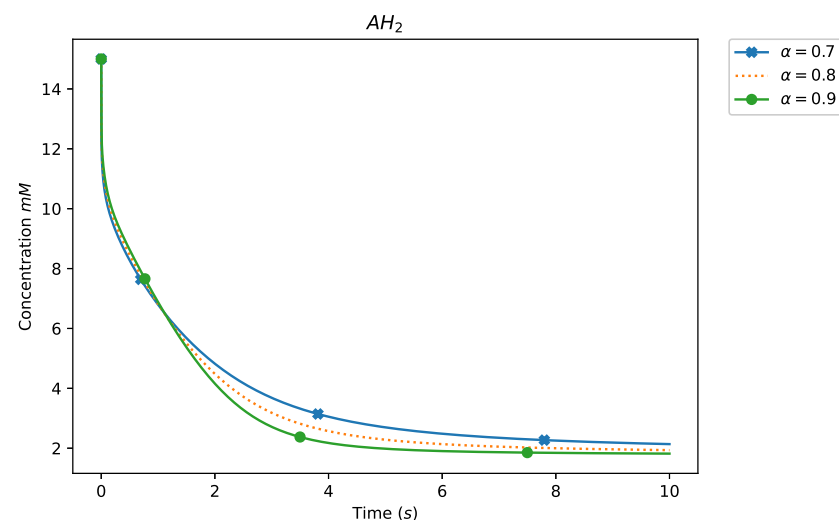


Figure 7. Numerical solutions of the model for the concentration of AH_2 . Each line represents the concentration of AH_2 in the mixture with respect to t for different values $\alpha = 0.7$, $\alpha = 0.8$, and $\alpha = 0.9$. The values of the model parameters are in the main text. Similarly, the initial conditions of the model are also presented in the main text.

4. Conclusions

Peroxidase enzymes facilitate oxidation with the assistance of H_2O_2 to assist plants in maintaining optimal concentrations of organic compounds essential for physiological functions. The cellular regulation of the oxidation rates involves inhibiting the enzyme activity. Cells employ two inhibitory mechanisms to modulate enzyme activity: a noncompetitive substrate inhibition process and a competitive substrate inhibition process. This paper presents a fractional mathematical model elucidating the H_2O_2 -mediated oxidation catalysed by *Spanish broom peroxidase*. Our mathematical model serves to dissect the regulatory mechanisms governing the behaviour of Spanish broom peroxidase. The biological evidence utilised in the modeling process has been previously established. However, this study marks the first instance where these concepts have been synthesised into a fractional mathematical model. The model incorporates numerous bound states for the enzyme, along with their corresponding activation statuses. The model was numerically integrated

using the `fodeint`, from the SciPy Python library, and the solutions obtained were found to align with the established behaviour of *Spanish broom peroxidase*. Furthermore, the model output demonstrated sensitivity to the fractional order.

While the model developed in this study was thoroughly investigated, there exists potential for improvement and future research. For instance, one avenue for further exploration is the estimation of model parameters using experimental data. Additionally, within the confines of this study, we did not specifically examine the sensitivity of the model output to small variations in parameter values [44,45]. Consequently, employing the homotopy analysis method to derive analytic solutions for the model [46,47] may enhance the sensitivity analysis, as these analytic solutions could potentially reduce computational expenses. Furthermore, it may be of interest to conduct a research study aimed at developing a computational tool for numerically solving the model, based on the methods proposed in the referenced papers [42,43]. In addition, addressing the positivity of the solutions of the model is an important consideration [48]. Finally, a notable limitation of the study lies in the absence of validation against experimental data. While the theoretical and computational aspects were explored, the lack of empirical validation leaves room for further investigation and refinement.

Author Contributions: Conceptualisation, V.Q.M. and T.A.N.; Methodology, V.Q.M.; Software, V.Q.M.; Validation, T.A.N.; Formal Analysis, V.Q.M. and T.A.N.; Investigation, V.Q.M.; Data Curation, V.Q.M.; Writing—Original Draft Preparation, V.Q.M.; Writing—Review and Editing, T.A.N. and V.Q.M.; Visualisation, V.Q.M.; Supervision, V.Q.M.; Project Administration, V.Q.M.; Funding Acquisition, T.A.N. and V.Q.M. All authors have read and agreed to the published version of the manuscript.

Funding: This research has received no external funding.

Data Availability Statement: No new data were created or analyzed in this study. Data sharing is not applicable to this article.

Acknowledgments: The authors would like to thank Thu Dau Mot University for financial support. The authors thank the anonymous referees for their valuable suggestions that helped improve the report.

Conflicts of Interest: Vinh Q. Mai and Thái Anh Nhan declare that they have no conflicts of interest, financial or ethical, of any kind.

References

1. Bugg, T.D.H. *Introduction to Enzyme and Coenzyme Chemistry*; John Wiley & Sons: Hoboken, NJ, USA, 2012.
2. Cox, M.M.; Cox, M.M.; Lehninger, A.L.; Nelson, D.L. *Lehninger Principles of Biochemistry*; Macmillan: New York, NY, USA, 2005.
3. Frey, P.A.; Hegeman, A.D. *Enzymatic Reaction Mechanisms*; Oxford University Press: Oxford, UK, 2007.
4. Liu, D.M.; Dong, C. Recent advances in nano-carrier immobilized enzymes and their applications. *Process Biochem.* **2020**, *92*, 464–475. [[CrossRef](#)]
5. Radzicka, A.; Wolfenden, R. A proficient enzyme. *Science* **1995**, *267*, 90–93. [[CrossRef](#)] [[PubMed](#)]
6. Galende, P.P.; Cuadrado, N.H.; Kostetsky, E.Y.; Roig, M.G.; Villar, E.; Shnyrov, V.L.; Kennedy, J.F. Kinetics of Spanish broom peroxidase obeys a ping-pong bi-bi mechanism with competitive inhibition by substrates. *Int. J. Biol. Macromol.* **2015**, *81*, 1005–1011. [[CrossRef](#)] [[PubMed](#)]
7. Piwonski, H.M.; Gomanovsky, M.; Bensimon, D.; Horovitz, A.; Haran, G. Allosteric inhibition of individual enzyme molecules trapped in lipid vesicles. *Proc. Natl. Acad. Sci. USA* **2012**, *109*, E1437–E1443. [[CrossRef](#)] [[PubMed](#)]
8. Kirk, O.; Borchert, T.V.; Fuglsang, C.C. Industrial enzyme applications. *Curr. Opin. Biotechnol.* **2002**, *13*, 345–351. [[CrossRef](#)] [[PubMed](#)]
9. Chapman, J.; Ismail, A.E.; Dinu, C.Z. Industrial applications of enzymes: Recent advances, techniques, and outlooks. *Catalysts* **2018**, *8*, 238. [[CrossRef](#)]
10. Drauz, K.; Gröger, H.; May, O. *Enzyme Catalysis in Organic Synthesis*; 3 Volume Set; John Wiley & Sons: Hoboken, NJ, USA, 2012; Volume 1.
11. Okamoto, S.; Hijikata-Okunomiya, A.; Wanaka, K.; Okada, Y.; Okamoto, U. Enzyme-controlling medicines: Introduction. *Semin. Thromb. Hemost.* **1997**, *23*, 493–501. [[CrossRef](#)] [[PubMed](#)]
12. Azizyan, R.A.; Gevorgyan, A.E.; Arakelyan, V.B.; Gevorgyan, E.S. Mathematical modeling of bi-substrate enzymatic reactions with Ping-Pong mechanism in the presence of competitive inhibitors. *World Acad. Sci. Eng. Technol.* **2013**, *74*, 966–968.

13. Hermansyah, H.; Kubo, M.; Shibasaki-Kitakawa, N.; Yonemoto, T. Mathematical model for stepwise hydrolysis of triolein using candida rugosa lipase in biphasic oil-water system. *Biochem. Eng. J.* **2006**, *31*, 125–132. [[CrossRef](#)]
14. Mai, V.Q.; Nhan, T.A.; Hammouch, Z. A mathematical model of enzymatic non-competitive inhibition by product and its applications. *Phys. Scr.* **2021**, *96*, 124062. [[CrossRef](#)]
15. Mai, V.Q.; Vo, T.T.; Meere, M. Modelling hyaluronan degradation by streptococcus pneumoniae hyaluronate lyase. *Math. Biosci.* **2018**, *303*, 126–138. [[CrossRef](#)] [[PubMed](#)]
16. Mai, V.Q.; Meere, M. Modelling the phosphorylation of glucose by human hexokinase I. *Mathematics* **2021**, *9*, 2315. [[CrossRef](#)]
17. Segel, I.H. *Enzyme Kinetics: Behavior and Analysis of Rapid Equilibrium and Steady State Enzyme Systems*; Wiley: New York, NY, USA, 1975.
18. Doorn, W.G.V.; Ketsa, S. Cross reactivity between ascorbate peroxidase and phenol (guaiacol) peroxidase. *Postharvest Biol. Technol.* **2014**, *95*, 64–69. [[CrossRef](#)]
19. Dunford, H.B. *Heme Peroxidases*; John Wiley: Hoboken, NJ, USA, 1999.
20. Pozdnyakova, N.; Makarov, O.; Chernyshova, M.; Turkovskaya, O.; Jarosz-Wilkolazka, A. Versatile peroxidase of *Bjerkandera fumosa*: Substrate and inhibitor specificity. *Enzym. Microb. Technol.* **2013**, *52*, 44–53. [[CrossRef](#)] [[PubMed](#)]
21. Pérez Galende, P.; Manzano Muñoz, T.; Roig, M.G.; García de María, C.C. Use of crude extract of lentil plant (*Lens culinaris* Medikus) in peroxidase-based analyses: Fast kinetic determination of hydrogen peroxide and sarcosine in urine. *Anal. Bioanal. Chem.* **2012**, *404*, 2377–2385. [[CrossRef](#)] [[PubMed](#)]
22. Hidalgo, N.; Mangiameli, G.; Manzano, T.; Zhadan, G.G.; Kennedy, J.F.; Shnyrov, V.L.; Roig, M.G. Oxidation and removal of industrial textile dyes by a novel peroxidase extracted from post-harvest lentil (*Lens culinaris* L.) stubble. *Biotechnol. Bioprocess Eng.* **2011**, *16*, 821–829. [[CrossRef](#)]
23. Hilfer, R. *Applications of Fractional Calculus in Physics*; World Scientific: Singapore, 2000.
24. Ishteva, M. *Properties and Applications of the Caputo Fractional Operator*; Department of Mathematics, University of Karlsruhe: Karlsruhe, Germany, 2005; p. 5.
25. Kilbas, A.A.; Srivastava, H.M.; Trujillo, J.J. *Theory and Applications of Fractional Differential Equations*; Elsevier: Amsterdam, The Netherlands, 2006; Volume 204.
26. Miller, K.S.; Ross, B. *An Introduction to the Fractional Calculus and Fractional Differential Equations*; Wiley: New York, NY, USA, 1993.
27. Podlubny, I. *Fractional Differential Equations, Mathematics in Science and Engineering*; Academic Press: New York, NY, USA, 1999.
28. Rahimkhani, P.; Ordokhani, Y.; Babolian, E. Numerical solution of fractional pantograph differential equations by using generalized fractional-order Bernoulli wavelet. *J. Comput. Appl. Math.* **2017**, *309*, 493–510. [[CrossRef](#)]
29. Alicea, R.M. A mathematical model for enzyme kinetics multiple time scale analysis. *Asymptot. Perturbations A* **2010**, *2*, 1–9.
30. Alawneh, A. Application of the multistep generalized differential transform method to solve a time-fractional enzyme kinetics. In *Discrete Dynamics in Nature and Society*; Hindawi: London, UK, 2013.
31. Hu, Y.; He, J.H. On fractal space-time and fractional calculus. *Therm. Sci.* **2016**, *20*, 773–777. [[CrossRef](#)]
32. Mathai, A.M.; Haubold, H.J. *Fractional and Multivariable Calculus: Model Building and Optimization Problems*; Springer Optimization and Its Applications: Berlin/Heidelberg, Germany, 2017; p. 122.
33. Chang, C.H.; Cha, S.; Brockman, R.W.; Bennett, L.L., Jr. Kinetic studies of adenosine kinase from 11210 cells: A model enzyme with a two-site Ping-Pong mechanism. *Biochemistry* **1983**, *22*, 600–611. [[CrossRef](#)]
34. Cook, P.F.; Cleland, W.W. *Enzyme Kinetics and Mechanism*; Garland Science: New York, NY, USA, 2007.
35. Voit, E.O.; Martens, H.A.; Omholt, S.W. 150 years of the mass action law. *PLoS Comput. Biol.* **2015**, *11*, e1004012. [[CrossRef](#)] [[PubMed](#)]
36. Python Software Foundation. Available online: <https://www.python.org/> (accessed on 25 January 2024).
37. Aburn, M. Numerical Integration of Fractional Ordinary Differential Equations (FODE). Available online: <https://pypi.org/project/fodeint/> (accessed on 25 March 2023).
38. Numpy. Available online: <https://numpy.org/> (accessed on 25 January 2024).
39. Scipy Open Source Python Library. Available online: <https://www.scipy.org/> (accessed on 25 January 2024).
40. Diethelm, K.; Ford, N.J.; Freed, A.D. Detailed error analysis for a fractional Adams method. *Numer. Algorithms* **2004**, *36*, 31–52. [[CrossRef](#)]
41. Li, C.; Zeng, F. Finite difference methods for fractional differential equations. *Int. J. Bifurc. Chaos* **2012**, *22*, 1230014. [[CrossRef](#)]
42. Mahatekar, Y.; Scindia, P.S.; Kumar, P. A new numerical method to solve fractional differential equations in terms of Caputo-Fabrizio derivatives. *Phys. Scr.* **2023**, *98*, 024001. [[CrossRef](#)]
43. Shymanskyi, V.; Sokolovskyy, I.; Sokolovskyy, Y.; Bubnyak, T. Variational method for solving the time-fractal heat conduction problem in the Claydite-Block construction. In *International Conference on Computer Science, Engineering and Education Applications*; Springer International Publishing: Cham, Switzerland, 2022; pp. 97–106.
44. Saltelli, A.; Ratto, M.; Andres, T.; Campolongo, F.; Cariboni, J.; Gatelli, D.; Tarantola, S. *Global Sensitivity Analysis: The Primer*; John Wiley & Sons: Hoboken, NJ, USA, 2008.
45. Sobol, I.M. Global sensitivity indices for nonlinear mathematical models and their Monte Carlo estimates. *Math. Comput. Simul.* **2001**, *55*, 271–280. [[CrossRef](#)]
46. Alrabaiiah, H.; Ali, A.; Haq, F.; Shah, K. Existence of fractional order semianalytical results for enzyme kinetics model. *Adv. Differ. Equ.* **2020**, *443*, 1–13. [[CrossRef](#)]

47. Saratha, S.R.; Bagyalakshmi, M.; Sai Sundara Krishnan, G. Fractional generalised homotopy analysis method for solving nonlinear fractional differential equations. *Comput. Appl. Math.* **2020**, *39*, 112. [[CrossRef](#)]
48. Boulares, H.; Ardjouni, A.; Laskri, Y. Positive solutions for nonlinear fractional differential equations. *Positivity* **2017**, *21*, 1201–1212. [[CrossRef](#)]

Disclaimer/Publisher’s Note: The statements, opinions and data contained in all publications are solely those of the individual author(s) and contributor(s) and not of MDPI and/or the editor(s). MDPI and/or the editor(s) disclaim responsibility for any injury to people or property resulting from any ideas, methods, instructions or products referred to in the content.